ISSN 2075-1087, Gyroscopy and Navigation, 2024, Vol. 15, No.2, pp. 39-50.
Russian Text © The Author(s), 2024, published in Giroskopiya i Navigatsiya, 2024, No.2, pp. 66-84.

Astronomical Calibration of a Strapdown Astroinertial Navigation System. Part 1. Calibration of Mutual Attitude of Digital Cameras

N.N. Vasilyuk[a] (ORCID: 0000-0003-2317-8066), G.A. Nefedov[b], E.A. Sidorova[b], and N.A. Shagimuratova[b]

[a]*SPC Elektrooptika, LLC, Moscow, Russia,*
[b]*Ramensky Instrument Engineering Plant, Ramenskoye, Russia*
*****e-mail: nik-vasilyuk@yandex.ru*
Received December 13, 2023, reviewed March 29, 2024, accepted April 10, 2024

Abstract: Astronomical calibration refers to determination of the constant mutual attitude of digital cameras and the inertial measurement unit using ground-based star observations. The first part of this paper considers calibrating the attitude of all cameras relative to the selected one. The calibrated vector contains the useful parameters (three attitude angles of each camera relative to the selected one) and interfering parameters (three attitude angles of the selected camera in the Earth-fixed frame at the time of shooting each frame). The system of nonlinear equations for determining the calibrated vector is based on the differences in the coordinates of images of the identified stars, which are calculated in the image planes of different cameras for each frame and then combined into a common residual vector. Atmospheric refraction and velocity aberration of light are considered when projecting the identified stars from the star catalog onto the image plane. Before solving the system of equations, intrinsic parameters of each camera are determined. Calibrating the relative attitude of real cameras provides a virtual camera with an extended field of view, which significantly reduces the error in star-based attitude determination. A virtual camera error model is provided that takes into account the errors in astronomical calibration. The results from experimental verification show that the error in astronomical calibration of the cameras' relative attitude does not exceed 2 arcsec for each useful parameter.

Keywords: star tracker, calibration, strapdown astroinertial navigation system, refraction, aberration, distortion, intrinsic parameters.

1. INTRODUCTION

A strapdown astroinertial navigation system (AINS) consists of an optoelectronic astrovision unit (AVU), inertial measurement unit (IMU), and computer assembled into a single structure without moving parts. The computer determines the AINS attitude relative to the stars based on images of constellations received from the AVU. In this paper, we consider an AINS for navigation relative to the Earth, where AVU measurements are used to correct the continuously growing errors in the trajectory defined with the aid of strapdown inertial navigation system (SINS) [1, 2].

The IMU measures the projections of the absolute angular velocity and specific force vectors onto oblique bases formed by the triads of the sensitivity axes of gyroscopes and accelerometers. These measurements can be used for trajectory evaluation with the use of inertial dead-reckoning after reducing two oblique bases to the right-hand orthogonal measurement frame (MF). The MF axes directions are determined by matrices obtained by IMU calibration on rate tables. Navigation grade IMUs feature the RMS errors in calibration of the sensitivity axes relative to MF of 3 arcsec for gyroscopes and 15 arcsec for accelerometers [3]. The IMU performs navigation measurements with a high frequency and under any motion conditions, so MF is taken to be the measurement frame of the whole AINS [4].

The AVU consists of one or more digital star cameras mounted on the common base. The star images observed by each camera are applied to determine the coordinates of the star direction vectors relative to the right-hand orthogonal camera frame CF. For external meters, the CF axes are set using optical reflecting cubes rigidly fixed to the camera body. The attitude of the cube faces relative to CF is determined on special calibration test beds with an RMS of about 2 arcsec [5–7].

For an AVU consisting of one camera, the error in rotation angle about the camera optical axis is several times larger than the error in the tilt of the optical axis [8]. When the Sun gets into the camera field of view, observing the stars, and therefore determining the atti-

tude becomes impossible. If two cameras are used and there is no Sun, the differences in the accuracies of AVU rotation angles about different axes are eliminated. When the Sun gets into the field of view of one camera, the AVU retains its ability to determine its attitude due to the second one. Adding a third camera to the configuration solves both problems: the Sun may get into the field of view of one camera, but the other two will continue to observe the stars. For this, the fields of view of the three cameras should not overlap, and their optical axes should not lie in the same plane [9].

The AVU cameras are rigidly connected to the AINS structure and synchronized with its time scale, so AVU can be considered to be a kind of virtual camera with a complex spatially distributed field of view. The right-hand orthogonal virtual frame (VF), relative to which constant attitude parameters of CF of each real camera should be determined, is bound with the virtual camera [10, 11]. These parameters can be used to transform the star direction vectors obtained in different CFs of individual cameras to VF and form a common bundle of direction vectors in a single frame, which is considered the result of astronomical observations by the virtual camera. The stars are identified and the virtual camera attitude is determined from the coordinates of vectors inside the bundle. To apply the attitude of the virtual camera for correcting inertial errors, the VF attitude relative to MF should be determined [12].

Determining the VF attitude relative to MF in the AINS from direct measurements of the optical cubes attitude is not reasonable. This approach requires reserving the space inside the AINS for cubes arrangement and laying paths along which the cube faces will be observed. The VF attitude relative to MF should be determined after calibrating the assembled AINS. The AINS consists of sensors that measure different physical inputs, optical and mechanical, and thus should be calibrated when exposed to both types of inputs. For this purpose, the calibrated AINS should rotate relative to uniquely identified point light sources with the known angular coordinates observed by each AVU camera focused to infinity.

AINS can be roughly calibrated accurate to 0.1° on simple laboratory test beds using plane contrast images [13]. To enhance the calibration accuracy, special laboratory test beds equipped with a turntable and collimators placing the point light sources to infinity are required [14–16]. The collimators should maintain their attitude relative to the test bed foundation accurate to several arcsec throughout the calibration procedure. If the intrinsic parameters of individual cameras (focal length, coordinates of the main image point, distortion coefficients) are calibrated simultaneously with the AINS, the table faceplate rotations relative to the collimators should be measured accurate to several arcsec [17, 18].

As an alternative to using high-accuracy laboratory test beds with artificial light sources, AINS calibration by stars (astronomical calibration) can be performed. The star angular coordinates are determined accurate to 0.01 arcsec in modern star catalogs [19]. When observed from the Earth's surface, the star's apparent position fluctuates randomly (jitters) near some mean direction, which is systematically shifted relative to the catalog direction. Systematic displacements depend on the direction of observation and consist of atmospheric refraction of the order of 0-70 arcsec and relativistic aberration of light of the order of 0-20 arcsec. They are corrected using appropriate mathematical models [20, 21]. Random jitters of the visible directions cannot be eliminated with a priori models. The jitter standard deviation estimated in quiet atmosphere from the solar limb is about 1-3 arcsec [22, 23].

Another advantage of using stars as calibration test objects is their distribution over the celestial sphere. A fixed camera with a 10-15° field of view easily detects 10-50 stars against a clear night sky. Technically, it is very difficult to construct a laboratory test bed, where several connected cameras simultaneously observe the same number of point sources determined accurate to 1-3 arcsec during all AINS calibration rotations.

The literature mainly considers AINS astronomical calibration algorithms based on the extended Kalman filter (EKF), where the calibrated parameters of VF attitude relative to MF are contained in the EKF state vector. The filters differ only in the set of estimated parameters added to the state vector, and in the method of constructing the observation vector. These algorithms are used for AINS in-flight calibration, since the influence of the atmosphere on the measured coordinates of stars is clearly not taken into account in them [24, 25]. Other AINS online calibration algorithms are based on comparing the components of the spacecraft angular velocity vector during intensive maneuvering, measured by IMU gyroscopes and calculated from AVU astronomical measurements. The comparison can be performed in real time using EKF [26] and in post-processing mode by solving the

Wahba's problem from the accumulated values of the angular velocity vector [27, 28]. The attitude of VF relative to MF can be determined as the optimal transformation of rotation between two sets of synchronous attitude values calculated from the IMU and AVU measurements. The growing errors in the IMU inertial dead-reckoning are not taken into account in this case [29].

In this paper, AINS ground calibration is performed using a simple pan-and-tilt device. The calibration measurements are processed in batch mode without applying the EKF, which avoids the limitations of its physical realizability (causality) and excludes the analysis of convergence of the state vector a posteriori estimate to the steady-state value. The calibration algorithm is formulated for AINS, which includes a separately calibrated IMU, for which the matrices of sensitivity axes misalignment relative to MF are defined. This approach simplifies the AINS calibration procedure and reduces the number of estimated parameters.

Within the framework of the considered problem, AINS calibration motion is a sequence of static positions, between which short calibration turns are performed. In static positions, AINS rotates relative to the stars due to the Earth rotation. Due to the structure of inertial and optical measurements in AINS, calibration is divided into two successive steps. At the first step, the attitude of individual cameras relative to VF is determined from calibration measurements. This step is described in the first part of the paper and is further referred to as AVU astronomical calibration.

At the second step, the attitude of VF relative to MF (or of AVU relative to IMU) is determined from the same measurements. The second part will be devoted to this.

2. PROBLEM STATEMENT

2.1. Description of the Calibration Procedure

AINS astronomical calibration is performed on a clear starry night in the countryside, at the site with the known geographical coordinates: latitude B^{clb}, longitude L^{clb}, and altitude H^{clb}. The AINS time scale, relative to which inertial and astronomical measurements are conducted, is synchronized with the UTC (SU) time scale.

Coordinates of the calibration site can be determined and the time scale can be synchronized using the GNSS (GLONASS) receiver. In this case the positioning error in the horizontal plane in the code mode is $\sigma_{GLN} = 2.5$ m, which is equivalent to geographical coordinates error $\sigma_B \approx \sigma_{GLN} / R_\oplus = 0.08$ arcsec in latitude and $\sigma_L \approx \sigma_{GLN} / (R_\oplus \cos B^{MSK}) = 0.15$ arcsec, where $B^{MSK} = 56$ N – latitude of Moscow, and $R_\oplus = 6371$ km is the radius of the Earth. Synchronization error σ_{SNC} between AINS and UTC (SU) should not exceed $\sigma_{SNC} \le 1$ ms, and the Earth rotation angle error is $\sigma_\oplus \le \sigma_{SNC}$ 15 arcsec/s = 0.015 arcsec. These angular errors are small compared to other errors in the calibrated system and can be ignored.

An example of the calibrated AINS configuration is shown in Fig. 1. During calibration, arrays of frames with images of the starry sky from separate AVU digital cameras and IMU data are continuously recorded on an external data storage. Frame arrays are numbered in the order of receiving: $n = 1...N$, where N is the number of arrays obtained during the calibration. The digital cameras in AVU are synchronized with each other, and the array with number n contains the frames pertaining to the common time t_{En}, when the exposure of all cameras starts. The time interval between successive times t_{En} and t_{En+1} may vary. IMU performs inertial measurements at equidistant times $t_{Ik} = t_{I0} + kT_{IMU}$, where T_{IMU} is the constant IMU measurements period; t_{I0} is the initial time; $k \ge 0$ is the consecutive number of the IMU measurement counted from the initial measurement at t_{I0}. The digital values of t_{En} and t_{Ik} are set on the UTC (SU) time scale.

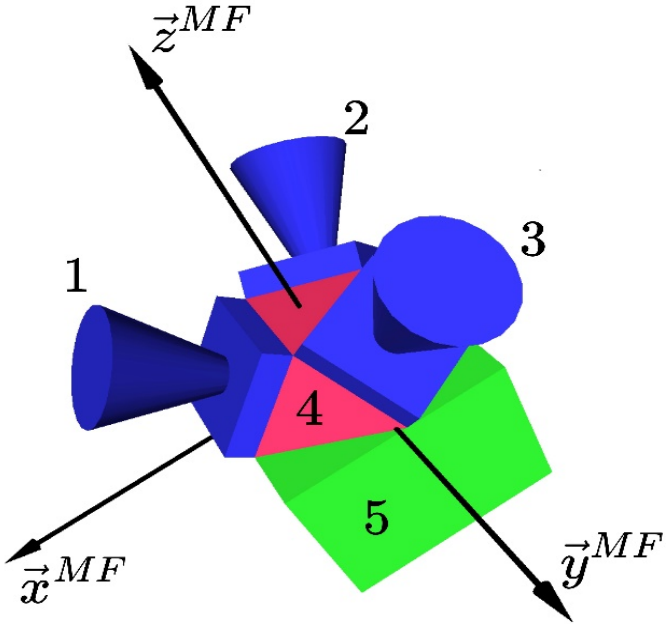

Fig. 1. Configuration of the calibrated AINS: *1*, *2*, *3* – digital cameras with the blends, *4* – AVU foundation, *5* – IMU.

During calibration, the AINS rotates to $p = 1...P$ different orientations, where it is held stationary rela-

tive to the Earth. These rotations are needed to calibrate AVU attitude relative to IMU, and they will be detailed in the second part of the paper. AINS attitude is controlled approximately, the measurements of angle sensors in the rotation axes of the pan-and-tilt device are not used in processing the calibration measurements. During the rotations AINS continues its operation, and data recording is not stopped.

In each calibration position, the AINS is installed so that all digital cameras can observe the stars without obstacles. Atmospheric refraction is taken into account using the plane-parallel atmosphere model, so the zenith angles of the optical axes of individual cameras in each position should not exceed 50° [20]. AINS rotations are optional, but useful for the calibration of relative attitude of AVU cameras discussed in the first part of the paper. They increase the variance of errors in star directions due to AINS bending deformation effects and errors in refraction and aberration compensation algorithms. These effects are not explicitly considered in AVU measurement error model. They are considered indirectly, by increasing the variances of the estimates of the calibrated parameters.

2.2. AVU Geometric Configuration and Calibrated Parameters

The attitudes of different frames are set using angles similar to heading ψ (clockwise), pitch ϑ, and roll γ, with the rotation matrices

$$\mathbf{R}_{\psi}(\alpha)=\begin{bmatrix} c_\alpha & s_\alpha & 0 \\ -s_\alpha & c_\alpha & 0 \\ 0 & 0 & 1 \end{bmatrix},\ \mathbf{R}_{\vartheta}(\alpha)=\begin{bmatrix} 1 & 0 & 0 \\ 0 & c_\alpha & -s_\alpha \\ 0 & s_\alpha & c_\alpha \end{bmatrix},$$

$$\mathbf{R}_{\gamma}(\alpha)=\begin{bmatrix} c_\alpha & 0 & s_\alpha \\ 0 & 1 & 0 \\ -s_\alpha & 0 & c_\alpha \end{bmatrix},$$

where $c_\alpha = \cos\alpha$, $s_\alpha = \sin\alpha$. The orthogonal matrix for vector coordinates transformation from the final frame *X2* to the initial one *X1* has the form:

$$\mathbf{C}_{X1}^{X2}=\begin{bmatrix} c_{11} & c_{12} & c_{13} \\ c_{21} & c_{22} & c_{23} \\ c_{31} & c_{32} & c_{33} \end{bmatrix}=\mathbf{R}_{\psi}(\psi)\mathbf{R}_{\vartheta}(\vartheta)\mathbf{R}_{\gamma}(\gamma)= \tag{1}$$

$$=\begin{bmatrix} c_\gamma c_\psi + s_\gamma s_\psi s_\vartheta & c_\vartheta s_\psi & c_\psi s_\gamma - c_\gamma s_\psi s_\vartheta \\ c_\psi s_\gamma s_\vartheta - c_\gamma s_\psi & c_\psi c_\vartheta & -s_\gamma s_\psi - c_\gamma c_\psi s_\vartheta \\ -c_\vartheta s_\gamma & s_\vartheta & c_\gamma c_\vartheta \end{bmatrix}.$$

The rotation angles from the matrix $\mathbf{C}_{X1}^{X2}$ coefficients are written as follows:

$$\vartheta = \arcsin c_{32},\ \psi=\begin{cases}\arccos(c_{22}/\cos\vartheta),\ c_{12}\ge 0\\ 2\pi-\arccos(c_{22}/\cos\vartheta),\ c_{12}<0\end{cases},$$

$$\gamma=\begin{cases}\arccos(c_{33}/\cos\vartheta),\ c_{31}\le 0\\ -\arccos(c_{33}/\cos\vartheta),\ c_{31}>0\end{cases}. \tag{2}$$

The AVU consists of $I \ge 1$ identical digital cameras. Each camera with the number $i = 1...I$ has its body-fixed frame CF^i The frame CF and the measurement model of the cameras are described in [30]. The attitude parameters of cameras relative to the AVU cannot be measured directly. Only the attitude of one camera relative to the other can be determined from the star observations, so CF^1 is selected to be VF, and the attitude angles $\alpha_\psi^i, \alpha_\vartheta^i, \alpha_\gamma^i$ of the remaining cameras $i = 2...I$ relative to camera 1 are calculated during the calibration. These angles define three successive rotations through the angles transforming VF to CF^i. The attitude of CF^1 relative to VF is written as $\alpha_\psi^1=\alpha_\vartheta^1=\alpha_\gamma^1=0$. For brevity, three rotation angles are written in vector form: $\boldsymbol{\alpha}^i=[\alpha_\psi^i\ \alpha_\vartheta^i\ \alpha_\gamma^i]^{\mathrm{T}}$. The purpose of AVU astronomical calibration is to determine 3 (I–1) useful parameters $\{\boldsymbol{\alpha}^i\}_{i=2}^I$.

During the astronomical calibration, the star observations are performed from the Earth's surface, from under the Earth's atmosphere. Atmospheric refraction distorts the star apparent zenith angle and should be considered in processing the calibration observations. To calculate the zenith angles of the observed stars, the camera attitude relative to the Earth should be determined. It cannot be measured directly, so it should be found from the calibration measurements.

The attitudes of individual cameras relative to the Earth cannot be considered constant, because calibration involves AINS rotations through large angles. Therefore, similarly to [31], three angles $\boldsymbol{\psi}_n = [\psi_n\ \vartheta_n\ \gamma_n]^{\mathrm{T}}$ of VF attitude relative to the Earth-fixed frame ENU (East–North–Up) bound with the calibration site are determined for each time point t_{En}. These angles form the $3N\times1$ vector $\boldsymbol{\psi}_\Sigma=[(\boldsymbol{\psi}_1)^{\mathrm{T}}\ ...\ (\boldsymbol{\psi}_N)^{\mathrm{T}}]^{\mathrm{T}}$ of interfering parameters.

Thus, calibration should provide determination of the $M\times1$ (M=3(N+I–1)) vector $\mathbf{x}=[\boldsymbol{\psi}_\Sigma^{\mathrm{T}}\ \boldsymbol{\alpha}^{2\mathrm{T}}\ ...\ \boldsymbol{\alpha}^{I\mathrm{T}}]^{\mathrm{T}}$ consisting of $M_I = 3N$ interfering parameters and $M_U = 3\ (I - 1)$ useful parameters.

3. PREPROCESSING OF CALIBRATION MEASUREMENTS

3.1. Transformation of the Measured Coordinates of Detected Stars

There are R_n^i detected and identified stars in each frame shot by the camera i and packed in array n. The total number of stars identified during calibration in all frames, received from camera i, is $R_\Sigma^i = \sum_{n=1}^{N} R_n^i$, in all frames, received from all cameras – $R_\Sigma = \sum_{i=1}^{I} R_\Sigma^i$. The stars are assigned consecutive numbers $r^i = 1...R_n^i$, and the raster coordinates $\{[\tilde{h}_{n,r^i}^i \ \tilde{w}_{n,r^i}^i]^\mathsf{T}\}_{r^i=1}^{R_n^i}$ of the brightness centers of their images are determined without distortion correction.

The raster coordinates $\{[\tilde{h}_{n,r^i}^i \ \tilde{w}_{n,r^i}^i]^\mathsf{T}\}_{r^i=1}^{R_n^i}$ are converted to the star direction vectors using a set of the camera intrinsic parameters $\mathbf{p}^i = [F^i \ h_O^i \ w_O^i \ k_1^i \ k_2^i]^\mathsf{T}$, where Fi is the focal length, $[h_O^i \ w_O^i]^\mathsf{T}$ are the raster coordinates of the principal point of the image, k_1^i, k_2^i are the radial distortion coefficients. The components of vector pi and their covariance matrix $\mathbf{P}_{\delta\mathbf{p}}^i$ are obtained during the camera factory calibration. If R_Σ^i is large enough, the current intrinsic parameters can be calculated directly from the processed measurements [31].

To calculate the bundle of direction vectors $\{\mathbf{s}_{CF^i\,n,r^i}^i\}_{r^i=1}^{R_n^i}$ of detected stars, the raster coordinates $\{[\tilde{h}_{n,r^i}^i \ \tilde{w}_{n,r^i}^i]^\mathsf{T}\}_{r^i=1}^{R_n^i}$ are first converted to vector coordinates with the corrected radial distortion:

$$\boldsymbol{\xi}_{n,r^i}^i \equiv \begin{bmatrix} x_{n,r^i}^i \\ y_{n,r^i}^i \end{bmatrix} = (1 + k_1^i |\tilde{\boldsymbol{\xi}}_{n,r^i}^i|^2 + k_2^i |\tilde{\boldsymbol{\xi}}_{n,r^i}^i|^4)\tilde{\boldsymbol{\xi}}_{n,r^i}^i,$$

where $\tilde{\boldsymbol{\xi}}_{n,r^i}^i = a[\tilde{h}_{n,r^i}^i - h_O^i \quad \tilde{w}_{n,r^i}^i - w_O^i]^\mathsf{T}$ are the vector coordinates without distortion correction; a is the side length of the square cell of the image sensor. Then, the direction vector coordinates relative to CF^i are calculated from the transformed vector coordinates:

$$\mathbf{s}_{CF^i\,n,r^i}^i = \frac{1}{(|\boldsymbol{\xi}_{n,r^i}^i|^2 + (F^i)^2)^{1/2}} \begin{bmatrix} -\boldsymbol{\xi}_{n,r^i}^i \\ F^i \end{bmatrix}.$$

3.2. Consideration for Aberration in Coordinates of Catalog Stars

To process the astronomical observations, the time t_{En} should be converted to Julian dates JD_n^{UT1} on UT1 (Universal Time) scale and JD_n^{TT} on TT (Terrestrial Time) scale [31]. The detected star r^i is considered identified if it corresponds to an entry in the star catalog (catalog star), which contains angular coordinates and their rates of change specified in the inertial Barycentric Celestial Reference System (BCRS) with its origin in the center of mass of the Solar System. The angular coordinates are used to calculate the bundle of direction vectors $\{\mathbf{b}_{BCRS\,n,r^i}^i\}_{r^i=1}^{R_n^i}$ of identified stars with Cartesian coordinates relative to BCRS at the time JD_n^{TT} [19].

The AVU observes stars from the surface of the Earth, which rotates about the Sun and about its axis. The relativistic aberration of light occurring during AVU motion relative to BCRS distorts the apparent star lines. This distortion reaches 20 arcsec, so relativistic aberration should be taken into consideration at the stage of preprocessing the calibration measurements by projecting vectors $\mathbf{b}_{BCRS\,n,r^i}^i$ onto the inertial Geocentric Celestial Reference System (GCRS), which moves with the Earth at the observation time JD_n^{TT} [21]:

$$\mathbf{g}_{GCRS\,n,r^i}^i = \left(1 + \frac{\mathbf{v}_{\oplus n}^\mathsf{T} \mathbf{b}_{BCRS\,n,r^i}^i}{c}\right)^{-1} \cdot$$

$$\cdot \left(\frac{\mathbf{b}_{BCRS\,n,r^i}^i}{\gamma_n} + \frac{\mathbf{v}_{\oplus n}}{c} + \frac{\gamma_n - 1}{\gamma_n} \frac{(\mathbf{v}_{\oplus n}^\mathsf{T} \mathbf{b}_{BCRS\,n,r^i}^i)\mathbf{v}_{\oplus n}}{v_{\oplus n}^2}\right)$$

where $\mathbf{v}_{\oplus n}$ is the velocity vector of the Earth's center of mass relative to BCRS at time JD_n^{TT} calculated from the Earth's ephemeris; $v_{\oplus n} = |\mathbf{v}_{\oplus n}|$; $\gamma_n = (1 - v_{\oplus n}^2 / c^2)^{-1/2}$; c is the speed of light in vacuum. The star direction vector $\mathbf{g}_{GCRS\,n,r^i}^i$ relative to GCRS takes into account the Earth's orbital motion only. Aberration caused by the Earth's diurnal rotation and the annual parallax of stars are not taken into account, which results in coordinate transformation error of maximum 1 arcsec [21].

3.3. Consideration of Atmospheric Refraction in Coordinates of Catalog Stars

Atmospheric refraction is taken into account by adding refractive distortions to the catalog vectors $\{\mathbf{g}_{GCRS\,n,r^i}^i\}_{r=1}^{R_n^i}$. To do this, first, each vector $\mathbf{g}_{GCRS\,n,r^i}^i$ is projected onto the International Terrestrial Reference

System (ITRS), which is tightly fixed with the Earth and participates in its diurnal rotation: $\mathbf{g}^i_{ITRS\,n,r^i} = \mathbf{S}^{GCRS}_{ITRS\,n}\mathbf{g}^i_{GCRS\,n,r^i}$. The coordinate transformation matrix $\mathbf{S}^{GCRS}_{ITRS}$ is calculated according to the methodological guidelines [32] at the time JD^{UT1}_n:

$$\mathbf{S}^{GCRS}_{ITRS\,n} = R^{pol}_n R^{rot}_n N^{nut}_n P^{prc}_n,$$

where R^{pol}_n is the displacement matrix of the Earth's instantaneous pole; R^{rot}_n is the matrix of the Earth's diurnal rotation, N^{nut}_n, P^{prc}_n are the nutation and precession matrices. Matrix R^{pol}_n is calculated from the angular coordinates of the Earth's instantaneous pole x_p, y_p at time JD^{UT1}_n taken from the Bulletin A of the International Earth Rotation Service. As of October 03, 2023, $x_p = 0.3003$ arcsec, $y_p = 0.3293$ arcsec.

The vector $\mathbf{g}^i_{ITRS\,n,r^i}$ is then projected onto the ENU with the coordinate transformation matrix $\mathbf{S}^{ITRS}_{ENU}$ calculated for the calibration site:

$$\mathbf{g}^i_{ENU\,n,r^i} = \mathbf{S}^{ITRS}_{ENU}\,\mathbf{g}^i_{ITRS\,n,r^i},$$

$$\mathbf{S}^{ITRS}_{ENU} = \begin{bmatrix} -\sin L^{clb} & \cos L^{clb} & 0 \\ -\sin B^{clb}\cos L^{clb} & -\sin B^{clb}\sin L^{clb} & \cos B^{clb} \\ \cos B^{clb}\cos L^{clb} & \cos B^{clb}\sin L^{clb} & \sin B^{clb} \end{bmatrix}.$$

Finally, the vector $\mathbf{g}^i_{ENU\,n,r^i}$ is distorted by atmospheric refraction. The result is the calculated direction vector $\mathbf{p}^i_{ENU\,n,r^i}$, in the direction of which the catalog star r^j is visible at the calibration site:

$$\mathbf{p}^i_{ENU\,n,r^i} = \frac{(\mathbf{I}_3 - \mathbf{u}\mathbf{u}^{\mathrm{T}})\mathbf{g}^i_{ENU\,n,r^i}}{n(H^{clb})} + \mathbf{u}\left(1 - \frac{1-(\mathbf{u}^{\mathrm{T}}\mathbf{g}^i_{ENU\,n,r^i})^2}{n(H^{clb})^2}\right)^{1/2},$$

where $\mathbf{u}^{\mathrm{T}} = [0\ 0\ 1]^{\mathrm{T}}$ is the local vertical direction in ENU; $n(H^{clb})$ is the refractive index in a plane-parallel model of the standard atmosphere at altitude H^{clb} [20].

4. CALCULATION OF CALIBRATED PARAMETERS

4.1. System of Equations for the Calibrated Parameters

The matrix $\mathbf{S}^{VF}_{ENU,n}$ of VF attitude relative to ENU and matrix $\mathbf{C}^{CF^i}_{VF}$ of CF^i attitude relative to VF are calculated by substituting $\boldsymbol{\psi}_n$ and $\boldsymbol{\alpha}^i$ to (1):

$$\begin{aligned} \mathbf{S}^{VF}_{ENU\,n} &= \mathbf{R}_\psi(\psi_n)\mathbf{R}_\vartheta(\vartheta_n)\mathbf{R}_\gamma(\gamma_n), \\ \mathbf{C}^{CF^i}_{VF} &= \mathbf{R}_\psi(\alpha^i_\psi)\mathbf{R}_\vartheta(\alpha^i_\vartheta)\mathbf{R}_\gamma(\alpha^i_\gamma). \end{aligned} \quad (3)$$

The matrix $\mathbf{S}^{CF^i}_{ENU,n} = \mathbf{S}^{VF}_{ENU\,n}\mathbf{C}^{CF^i}_{VF}$ of the camera i attitude relative to ENU projects the vector $\mathbf{p}^i_{ENU\,n,r^i}$ onto CF^i:

$$\mathbf{p}^i_{n,r^i} \equiv [p^i_{x\,n,r^i}\ \ p^i_{y\,n,r^i}\ \ p^i_{z\,n,r^i}]^{\mathrm{T}} = (\mathbf{S}^{CF^i}_{ENU,n})^{\mathrm{T}}\mathbf{p}^i_{ENU\,n,r^i}.$$

The vector coordinates of catalog stars are calculated from $\mathbf{p}^i_{n,r^i}$:

$$\hat{\boldsymbol{\xi}}^i_{n,r^i}(\boldsymbol{\psi}_n,\boldsymbol{\alpha}^i) = \begin{bmatrix} \hat{x}^i_{n,r^i} \\ \hat{y}^i_{n,r^i} \end{bmatrix} = -\frac{F^i}{p^i_{z\,n,r^i}}\begin{bmatrix} p^i_{x\,n,r^i} \\ p^i_{y\,n,r^i} \end{bmatrix}.$$

The $2R^i_n \times 1$ residual vector is formed from all the stars detected by camera i at time t_{En}:

$$\mathbf{f}^i_n(\boldsymbol{\psi}_n,\boldsymbol{\alpha}^i) \equiv \begin{bmatrix} \hat{\boldsymbol{\xi}}^i_{n,1}(\boldsymbol{\psi}_n,\boldsymbol{\alpha}^i) - \boldsymbol{\xi}^i_{n,1} \\ \vdots \\ \hat{\boldsymbol{\xi}}^i_{n,R^i_n}(\boldsymbol{\psi}_n,\boldsymbol{\alpha}^i) - \boldsymbol{\xi}^i_{n,R^i_n} \end{bmatrix}.$$

The residuals $\{\mathbf{f}^i_n(\boldsymbol{\psi}_n,\boldsymbol{\alpha}^i)\}^N_{n=1}$ are combined into a common $2R^i_\Sigma \times 1$ vector for all frames $n = 1\ldots N$ read from camera i:

$$\mathbf{f}^i(\boldsymbol{\psi}_\Sigma,\boldsymbol{\alpha}^i) \equiv [\mathbf{f}^i_1(\boldsymbol{\psi}_n,\boldsymbol{\alpha}^i)^{\mathrm{T}}\ \ldots\mathbf{f}^i_N(\boldsymbol{\psi}_N,\boldsymbol{\alpha}^i)^{\mathrm{T}}]^{\mathrm{T}}.$$

Combining the residual vectors for all cameras provides the final notation of the $2R_\Sigma \times 1$ system of equations for finding the calibrated parameters:

$$\mathbf{o}_{2R_\Sigma} = \mathbf{f}_\Sigma(\mathbf{x}), \quad (4)$$

where $\mathbf{f}_\Sigma(\mathbf{x}) = [\mathbf{f}^1(\boldsymbol{\psi}_\Sigma,\boldsymbol{\alpha}^1)^{\mathrm{T}}\ \ldots\ \mathbf{f}^I(\boldsymbol{\psi}_\Sigma,\boldsymbol{\alpha}^I)^{\mathrm{T}}]^{\mathrm{T}}$; $\mathbf{o}_M$ is a $M \times 1$ zero vector.

4.2. Solving the System of Equations

The system of equations (4) is inconsistent, because it contains parameters that are measured with errors. The system can be solved approximately with the iterative nonlinear least squares method (LSM) [33]. The components $[x_{M_I+3(i-2)+1,0}\ x_{M_I+3(i-2)+2,0}\ x_{M_I+3(i-2)+3,0}]^{\mathrm{T}}$, $i = 2\ldots I$ of the initial vector of calibrated parameters $\mathbf{x}_0$ for the angles $\boldsymbol{\alpha}^i$ are initialized with their nominal values set when designing the AVU. To initialize the components $[x_{3(n-1)+1,0}\ x_{3(n-1)+2,0}\ x_{3(n-1)+3,0}]^{\mathrm{T}}$ for the angles $\boldsymbol{\psi}_n$ for each frame $n = 1\ldots N$ of camera 1, the Wahba's problem [34] is solved between the vector bundles $\{\mathbf{p}^1_{n,r^1}\}^{R^1_n}_{r^1=1}$ and $\{\mathbf{s}^1_{CF^1\,n,r^1}\}^{R^1_n}_{r^1=1}$. The solution immediately provides the matrix $\mathbf{S}^{VF}_{ENU\,n}$, from which the initial values of the angles $\boldsymbol{\psi}_n$ are calculated according to (2).

To find the estimate $\mathbf{x}_j$ of the vector of calibrated parameters at the current iteration $j \geq 1$, formula (4) is linearized in the neighborhood of the estimate $\mathbf{x}_{j-1}$ obtained at the previous iteration j–1:

$$\mathbf{o}_{2R_\Sigma} \approx \mathbf{f}_{\Sigma,j-1} + \mathbf{H}_{j-1}\delta\mathbf{x}_j, \qquad (5)$$

where $\mathbf{f}_{\Sigma,j-1} = \mathbf{f}_\Sigma(\mathbf{x}_{j-1})$; $\delta\mathbf{x}_j$ is the vector of corrections to the estimate $\mathbf{x}_{j-1}$; $\mathbf{H}_{j-1} = [\mathbf{h}_{1,j-1} \ldots \mathbf{h}_{M,j-1}]$ is the Jacobian matrix for the function $\mathbf{f}_\Sigma(\mathbf{x})$ at the point $\mathbf{x}_{j-1}$; $\mathbf{h}_{m,j-1}$ is the Jacobian column with the number $m = 1 \ldots M$:

$$\mathbf{h}_{m,j-1} = \frac{\mathbf{f}_\Sigma(\mathbf{x}_{j-1} + 0.5d\mathbf{x}_m) - \mathbf{f}_\Sigma(\mathbf{x}_{j-1} - 0.5d\mathbf{x}_m)}{dx}.$$

Here $d\mathbf{x}_m = [\overset{1}{0}\ \overset{2}{0} \ldots \overset{m}{dx} \ldots \overset{M}{0}]$ is the increment for calculating the partial derivative with respect to the m coordinate; dx is the numerical differentiation step. The estimate $\mathbf{x}_j$ is calculated from (5) with a linear LSM:

$$\mathbf{x}_j = \mathbf{x}_{j-1} + \delta\mathbf{x}_j,\ \delta\mathbf{x}_j = -(\mathbf{H}_{j-1}^{\mathrm{T}}\mathbf{H}_{j-1})^{-1}\mathbf{H}_{j-1}^{\mathrm{T}}\mathbf{f}_{\Sigma,j-1}.$$

The iterative process stops at the iteration with the number J, for which $|\delta\mathbf{x}_J| = (\delta\mathbf{x}_J^{\mathrm{T}}\delta\mathbf{x}_J)^{1/2} \leq tr$, where $tr = 10^{-9}$ rad or 2×10^{-4} arcsec is the low preset threshold for stopping the iterative process. The value of $\mathbf{f}_{\Sigma,J}$ is used to calculate the covariance matrix of estimate $\mathbf{x}_j$:

$$\mathbf{P}_\mathbf{x} = \| p_{q,s} \|_{q,s=1}^{M} = \frac{\mathbf{f}_{\Sigma,J}^{\mathrm{T}}\mathbf{f}_{\Sigma,J}}{2R_\Sigma}(\mathbf{H}_J^{\mathrm{T}}\mathbf{H}_J)^{-1}.$$

The calibration provides the useful components of the vector $\mathbf{x}_\mathrm{j}$:

$$\boldsymbol{\alpha}^i = [x_{M_1+3(i-2)+1,J}\ x_{M_1+3(i-2)+2,J}\ x_{M_1+3(i-2)+3,J}]^{\mathrm{T}}$$

and the corresponding diagonal blocks of the 3×3 covariance matrix $\mathbf{P}_\mathbf{x}$:

$$\mathbf{P}_{\boldsymbol{\alpha}}^i = \begin{bmatrix} \sigma_{\alpha\psi i}^2 & * & * \\ * & \sigma_{\alpha\vartheta i}^2 & * \\ * & * & \sigma_{\alpha\vartheta i}^2 \end{bmatrix} = \| p_{M_1+3(i-2)+q,M_1+3(i-2)+s} \|_{q,s=1}^{3},$$

where $\sigma_{\alpha\psi i}^2, \sigma_{\alpha\vartheta i}^2, \sigma_{\alpha\vartheta i}^2$, are the variances of angles in the vector $\boldsymbol{\alpha}^\mathrm{i}$ described by the numbers of the order of 10^{-11}; * are the matrix elements with no special notation indicated with numbers of the order of $10^{-12} \ldots 10^{-11}$. Elements of the matrix $\mathbf{P}_\mathbf{x}$ describing cross-correlations between vectors $\boldsymbol{\alpha}^\mathrm{i}$ with different i are expressed with numbers of the order of $10^{-14} \ldots 10^{-13}$. These elements are further considered small and are not taken into account in the calculations.

5. AVU ERROR MODEL

The error model for a star tracker with one digital camera is constructed in [30]. In the present paper this model is generalized for an AVU considered as a virtual camera with a complex field of view due to the presence of several real digital cameras. The AVU attitude measured with the virtual camera at the current time is determined using only the synchronous images of the starry sky obtained by real cameras at the same time.

Let the array $\{\mathbf{s}_{CF^i\,r^i}^i\}_{r^i=1}^{R^i}$ of direction vectors of identified stars be detected from the image obtained by the camera $i = 1 \ldots I$. For each direction vector with the number $r^i = 1 \ldots R^i$, the error vector can be written in the form [30, formula (9)]:

$$\delta\tilde{\mathbf{s}}_{CF^i\,r^i}^i = \frac{\mathbf{I}_3 - \mathbf{s}_{CF^i\,r^i}^i(\mathbf{s}_{CF^i\,r^i}^i)^{\mathrm{T}}}{((x_{r^i}^i)^2 + (y_{r^i}^i)^2 + (F^i)^2)^{1/2}}(\mathbf{G}_1^{r^i}\delta\boldsymbol{\eta}_{ns}^{r^i} + \mathbf{G}_2^{r^i}\delta\boldsymbol{\varphi}^{r^i} + \mathbf{G}_3^{r^i}\delta\mathbf{p}^i),$$

where $[x_{r^i}^i\ y_{r^i}^i]^{\mathrm{T}}$ are the vector coordinates of the brightness center of the star image; F^i is the lens focal length; $\delta\boldsymbol{\varphi}^{r^i}$ is the vector of fluctuations of the star angular coordinates in turbulent atmosphere with covariance matrix $\sigma_{sh}^2\mathbf{I}_2$; σ_{sh}^2 is the variance of fluctuations of each coordinate; $\delta\boldsymbol{\eta}_{ns}^{r^i}$ is the error vector of the star vector coordinates with covariance matrix $\mathbf{P}_{ns}^{r^i}$; $\delta\mathbf{p}^i$ is the error vector of calibration of the camera i intrinsic parameters with covariance matrix $\mathbf{P}_{\delta\mathbf{p}}^i$; $\mathbf{G}_1^{r^i}$, $\mathbf{G}_2^{r^i}$, $\mathbf{G}_3^{r^i}$ are the distribution matrices of errors introduced by the components of the measurement model of the components of the star direction vector [30, formula (9)]. The presence of the AVU VF frame does not affect the notation for $\delta\tilde{\mathbf{s}}_{CF^i\,r^i}^i$.

The attitude matrix $\mathbf{C}_{VF}^{CF^i}$ for the camera i is calculated based on the calibration results $\boldsymbol{\alpha}^\mathrm{i}$ with an error $\delta\boldsymbol{\alpha}^\mathrm{i}$:

$$\mathbf{C}_{VF}^{CF^i} = \breve{\mathbf{C}}_{VF}^{CF^i}(\mathbf{I}_3 + [\delta\boldsymbol{\alpha}^i\times]),$$

where $\breve{\mathbf{C}}_{VF}^{CF^i}$ is the true projection matrix; $[\delta\boldsymbol{\alpha}^\mathrm{i}\times]$ is a skew-symmetric matrix consisting of the components of the vector $\delta\boldsymbol{\alpha}^\mathrm{i}$ when substituting it from the left side into a vector product of the form $\mathbf{a}\times\mathbf{b} = [\mathbf{a}\times]\mathbf{b}$,

$$[\mathbf{a}\times] = \begin{bmatrix} 0 & -a_z & a_y \\ a_z & 0 & -a_x \\ -a_y & a_x & 0 \end{bmatrix}.$$

In a virtual camera, a combined bundle $\{\mathbf{s}_{VF\,r}\}_{r=1}^{R^{tot}}$ of direction vectors is formed by projecting all vectors $\{\{\mathbf{s}^i_{CF^i\,r^i}\}_{r^i=1}^{R^i}\}_{i=1}^{I}$ onto VF:

$$\mathbf{s}_{VF\,r} = \mathbf{C}_{VF}^{CF^i}\,\mathbf{s}^i_{CF^i\,r^i} = \\ = \breve{\mathbf{C}}_{VF}^{CF^i}\,\breve{\mathbf{s}}^i_{CF^i\,r^i} + \breve{\mathbf{C}}_{VF}^{CF^i}\,(\delta\tilde{\mathbf{s}}^i_{CF^i\,r^i} - [\breve{\mathbf{s}}^i_{CF^i\,r^i}\times]\delta\boldsymbol{\alpha}^i),$$

where $R^{tot} = \sum_{i=1}^{I} R^i$ is the total number of stars detected and identified by all cameras at the current time; $r = r^i + \sum_{q=1}^{i-1} R^q$ is the consecutive number of the star r^i in the bundle. This shows that when shifting from a real camera to a virtual one, a new error term is added to the vector $\delta\tilde{\mathbf{s}}^i_{CF^i\,r^i}$, associated with the calibration error of the attitude of the real camera relative to VF. To account for this term, we introduce the effective error in determining the star direction vector by a certain AVU camera, which considers the VF frame:

$$\delta\mathbf{s}^i_{CF^i\,r^i} = \begin{cases} \delta\tilde{\mathbf{s}}^i_{CF^i\,r^i},\ i=1; \\ \delta\tilde{\mathbf{s}}^i_{CF^i\,r^i} - [\breve{\mathbf{s}}^i_{CF^i\,r^i}\times]\delta\boldsymbol{\alpha}^i,\ i=2...I. \end{cases}$$

The formula for the AVU error generalizes [30, formula (10)] written for the error vector for a single-camera star tracker to the case of I connected cameras:

$$\boldsymbol{\theta} = -\mathbf{K}\sum_{i=1}^{I}\mathbf{C}_{VF}^{CF^i}\sum_{r^i=1}^{R^i}[\mathbf{s}^i_{CF^i\,r^i}\times]\delta\mathbf{s}^i_{CF^i\,r^i} = \boldsymbol{\varepsilon} + \mathbf{b}_{int} + \mathbf{b}_{att},$$

where $\mathbf{K}$ is the 3×3 matrix coefficient calculated from the bundle $\{\mathbf{s}_{VF\,r}\}_{r=1}^{R^{tot}}$ of direction vectors; $\boldsymbol{\varepsilon} = -\mathbf{K}\sum_{i=1}^{I}\mathbf{C}_{VF}^{CF^i}\boldsymbol{\varepsilon}^i$ is AVU fluctuation error consisting of fluctuation errors $\{\boldsymbol{\varepsilon}^i\}_{i=1}^{I}$ of individual cameras with covariance matrices $\{\mathbf{P}^i_{\boldsymbol{\varepsilon}}\}_{i=1}^{I}$:

$$\boldsymbol{\varepsilon}^i = \sum_{r^i=1}^{R^i}\frac{[\mathbf{s}^i_{CF^i\,r^i}\times](\mathbf{G}_1^{r^i}\delta\boldsymbol{\eta}_{ns}^{r^i} + \mathbf{G}_2^{r^i}\delta\boldsymbol{\varphi}^{r^i})}{((x^i_{r^i})^2 + (x^i_{r^i})^2 + (F^i)^2)^{1/2}},$$

$$\mathbf{P}^i_{\boldsymbol{\varepsilon}} \equiv \mathrm{cov}\{\boldsymbol{\varepsilon}^i\} = \\ = -\sum_{r^i=1}^{R^i}\frac{[\mathbf{s}^i_{CF^i\,r^i}\times](\mathbf{G}_1^{r^i}\mathbf{P}_{ns}^{r^i}\mathbf{G}_1^{r^i\mathsf{T}} + \sigma_{sh}^2\mathbf{G}_2^{r^i}\mathbf{G}_2^{r^i\mathsf{T}})[\mathbf{s}^i_{CF^i\,r^i}\times]}{(x^i_{r^i})^2 + (y^i_{r^i})^2 + (F^i)^2}.$$

AVU systematic error $\mathbf{b}_{int} = -\mathbf{K}\sum_{i=1}^{I}\mathbf{C}_{VF}^{CF^i}\mathbf{b}^i_{int}$ consists of systematic errors $\{\mathbf{b}^i_{int}\}_{i=1}^{I}$ (with covariance matrices $\{\mathbf{P}^i_{int}\}_{i=1}^{I}$), which consider the errors in intrinsic parameters calibration for individual cameras:

$$\mathbf{b}^i_{int} = \sum_{r^i=1}^{R^i}\frac{[\mathbf{s}^i_{CF^i\,r^i}\times]\mathbf{G}_3^{r^i}\delta\mathbf{p}^i}{((x^i_{r^i})^2 + (x^i_{r^i})^2 + (F^i)^2)^{1/2}},$$

$$\mathbf{P}^i_{int} \equiv \mathrm{cov}\{\mathbf{b}^i_{int}\} = -\sum_{r^i=1}^{R^i}\frac{[\mathbf{s}^i_{CF^i\,r^i}\times]\mathbf{G}_3^{r^i}\mathbf{P}^i_{\delta\mathbf{p}}\mathbf{G}_3^{r^i\mathsf{T}}[\mathbf{s}^i_{CF^i\,r^i}\times]}{(x^i_{r^i})^2 + (y^i_{r^i})^2 + (F^i)^2}.$$

AVU systematic error $\mathbf{b}_{att} = -\mathbf{K}\sum_{i=2}^{I}\mathbf{C}_{VF}^{CF^i}\mathbf{b}^i_{att}$ consists of the systematic errors $\{\mathbf{b}^i_{att}\}_{i=1}^{I}$ (with covariance matrices $\{\mathbf{P}^i_{att}\}_{i=1}^{I}$), which consider the errors in calibration of the cameras' relative attitude within the AVU:

$$\mathbf{b}^i_{att} = -\sum_{r^i=1}^{R^i}\frac{[\mathbf{s}^i_{CF^i\,r^i}\times]^2\delta\boldsymbol{\alpha}^i}{((x^i_{r^i})^2 + (x^i_{r^i})^2 + (F^i)^2)^{1/2}},$$

$$\mathbf{P}^i_{att} \equiv \mathrm{cov}\{\mathbf{b}^i_{att}\} = \sum_{r^i=1}^{R^i}\frac{[\mathbf{s}^i_{CF^i\,r^i}\times]^2\mathbf{P}^i_{\boldsymbol{\alpha}}[\mathbf{s}^i_{CF^i\,r^i}\times]^2}{((x^i_{r^i})^2 + (y^i_{r^i})^2 + (F^i)^2)^{1/2}}.$$

$\mathbf{P}_{\boldsymbol{\theta}}$ is the covariance matrix of the attitude error for a multiple-camera AVU:

$$\mathbf{P}_{\boldsymbol{\theta}} = \mathbf{K}\left(\sum_{i=1}^{I}\mathbf{C}_{VF}^{CF^i}\left[\mathbf{P}^i_{\boldsymbol{\varepsilon}} + \mathbf{P}^i_{int} + \mathbf{P}^i_{att}\right](\mathbf{C}_{VF}^{CF^i})^{\mathsf{T}}\right)\mathbf{K}. \quad (6)$$

6. EXPERIMENTAL RESULTS

To experimentally test the algorithm, we used the AVU with $I = 3$ identical digital cameras with a nominal focal length F = 106 mm and pixel size a = 6.9 microns (the pixel angular size a/F = 13.4 arcsec). In a calibration session lasting about 30 minutes, individual cameras have detected and identified $R^1_\Sigma = 3265$, $R^2_\Sigma = 1731$, $R^3_\Sigma = 2681$ stars with magnitudes ranging from 1.65 to 10.62. In total, $R\Sigma$ = 7677 stars were detected with all cameras.

The identified stars were first used to calibrate the intrinsic parameters of each camera separately according to the method [31]. Residual errors calculated in the image plane of each camera after calibration are shown in Fig. 2a. The residual errors were calculated for each identified star as the distance between the brightness center of its image (after distortion correction) and the projection of the catalog direction vector of this star on the image plane of the image sensor.

Then, the identified stars and calibrated intrinsic parameters were used to calibrate the relative attitude of the AVU cameras. The indicator of the calibration quality, as in the previous case, is the distance between the brightness centers of images of stars with numbers $r = 1...R\Sigma$ and the projections of their catalog direction vectors on the image planes of the image sensors:

$$d_r = \sqrt{\mathbf{f}_{\Sigma,J}(2r-1)^2 + \mathbf{f}_{\Sigma,J}(2r)^2} \,/\, a \text{, [pxl]},$$

where $\mathbf{f}_{\Sigma,J}(k)$ is the scalar component with number $k = 1...2R_\Sigma$ in the vector $\mathbf{f}_{\Sigma,J}$ of dimension $2R_\Sigma \times 1$. The values of d_r for a fixed number of iterations $J = 10$ are shown in Fig. 2b. The meaning of d_r is a residual for the identified star r remaining after the calibration of the cameras' relative attitude. From Figs. 2 a and b, the residual in the calibration of the relative attitude of the AVU cameras is limited by the residual in the calibration of the intrinsic parameters for each camera.

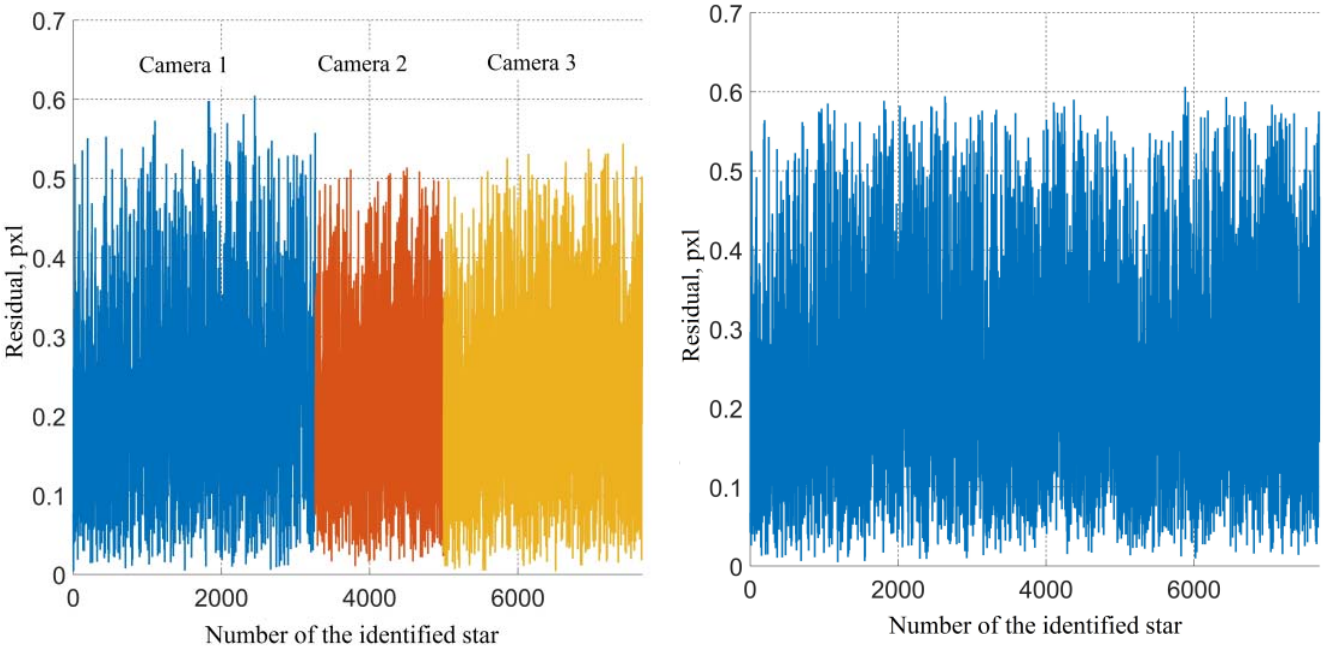

a) *b)*

Fig. 2. Residual errors after the calibrations: *a)* residuals after calibration of the intrinsic parameters of individual cameras; *b)* residuals after calibration of the relative attitude of the AVU cameras.

RMS deviations of cameras' relative attitudes calculated after AVU astronomical calibration from the diagonal elements of the matrices $\mathbf{P}_{\boldsymbol{\alpha}}^{i}$, $i = 2, 3$ are given in the Table. Within one session, the camera relative attitude angles are calibrated with an RMS of no more than 2 arcsec.

Table. Results of AVU astronomical calibration

i	$\sigma_{\alpha\psi i}$	$\sigma_{\alpha\vartheta i}$	$\sigma_{\alpha\gamma i}$
2	0.8 arcsec	0.8 arcsec	0.2 arcsec
3	1.6 arcsec	0.1 arcsec	1.2 arcsec

The calibrated AVU can determine the VF attitude at time t_{En} from the observations of a single camera, any pair of cameras, and all three cameras. The attitude errors for the same number of stars $R = 4$ ... 17 observed by different camera configurations can be demonstrated on the processed calibration measurements.

To demonstrate the AVU attitude errors with a single camera with the number $i = 1, 2, 3$, R brightest stars are selected in each frame obtained at time t_{En}. The direction vectors of these stars defined in CF^i are projected onto VF with the matrix $\mathbf{C}_{VF}^{CF^i}$ calculated using the calibrated angles $\boldsymbol{\alpha}^i$. For sets of projected vectors, the Wahba's problem is solved and the calculated attitude matrix $\mathbf{S}_{ENU\,n}^{VF\,\{i\}}(R)$ for one camera is determined.

To demonstrate the attitude errors for several cameras, we consider double {1,2}, {1,3}, {2,3} and triple {1,2,3} camera configurations. All the stars detected in the frames obtained at time t_{En} by each camera from the configuration are combined into a common array ranked in descending order of star brightness (in ascending order of magnitude). From the ranked array, the first R stars are selected, which are the brightest among the stars detected with this camera configuration. In the case of multiple cameras, R is the number of the stars selected for all cameras of the configuration rather than for each one separately. The direction vectors of these stars are projected onto VF. The Wahba's problems are solved for the vector sets, and three estimated attitude matrices $\mathbf{S}_{ENU\,n}^{VF\,\{1,2\}}(R)$, $\mathbf{S}_{ENU\,n}^{VF\,\{1,3\}}(R)$, $\mathbf{S}_{ENU\,n}^{VF\,\{2,3\}}(R)$ for dual configurations

{1,2},{1,3}, {2,3}, and matrix $\mathbf{S}_{ENU\,n}^{VF\,\{1,2,3\}}(R)$ for the triple configuration {1,2,3} are obtained.

The vector of calibrated parameters contains three VF attitude angles $\boldsymbol{\psi}_n = [\psi_n\ \vartheta_n\ \gamma_n]^{\mathrm{T}}$ for each time point t_{En}. For demonstration purposes, these angles determined with RMS deviation of the order of 1 arcsec can be taken to be true and the *true* matrix of VF attitude relative to ENU $\breve{\mathbf{S}}_{ENU\,n}^{VF}$ can be found according to (3). The angular error $\theta_n^{\{X\}}(R)$ in AVU attitude relative to ENU from R brightest stars at time t_n is given by

$$\theta_n^X(R) = \arccos\left(0{,}5[\ \mathrm{tr}\,(\mathbf{S}_{ENU\,n}^{VF\,X}(R)^{\mathrm{T}}\breve{\mathbf{S}}_{ENU\,n}^{VF}) - 1]\right),$$
$$X = \{1\};\{2\};\{3\};\{1,2\};\{1,3\};\{2,3\};\{1,2,3\}.$$

The mathematical expectation of the angular error $\theta^X(R)$ for various R is assumed to be zero. Therefore, the estimate $\sigma^X(R)$ of the RMS deviation of angular error is found by averaging over all processed frames without calculating the expected value:

$$\sigma^X(R) = \sqrt{\frac{\sum_{n=1}^{N}(\theta_n^{\{X\}}(R))^2}{N}}.$$

AVU attitude errors with the same number of stars observed by different camera configurations are shown in Fig. 3. In a single-camera configuration, R stars are observed by each camera separately. In double and triple configurations, R is the total number of stars observed by two and three cameras. As seen from the plots, adding a second camera significantly reduces the attitude error. The attitude errors for two and three cameras with the same number of stars slightly differ from each other. In a three-camera configuration, R brightest stars among all the stars detected by three cameras can be concentrated in the fields of view of only two cameras. In these cases, the triple configuration actually becomes a double one. If R brightest stars are distributed over the fields of view of three cameras, it provides a slightly lower error compared to the double configuration.

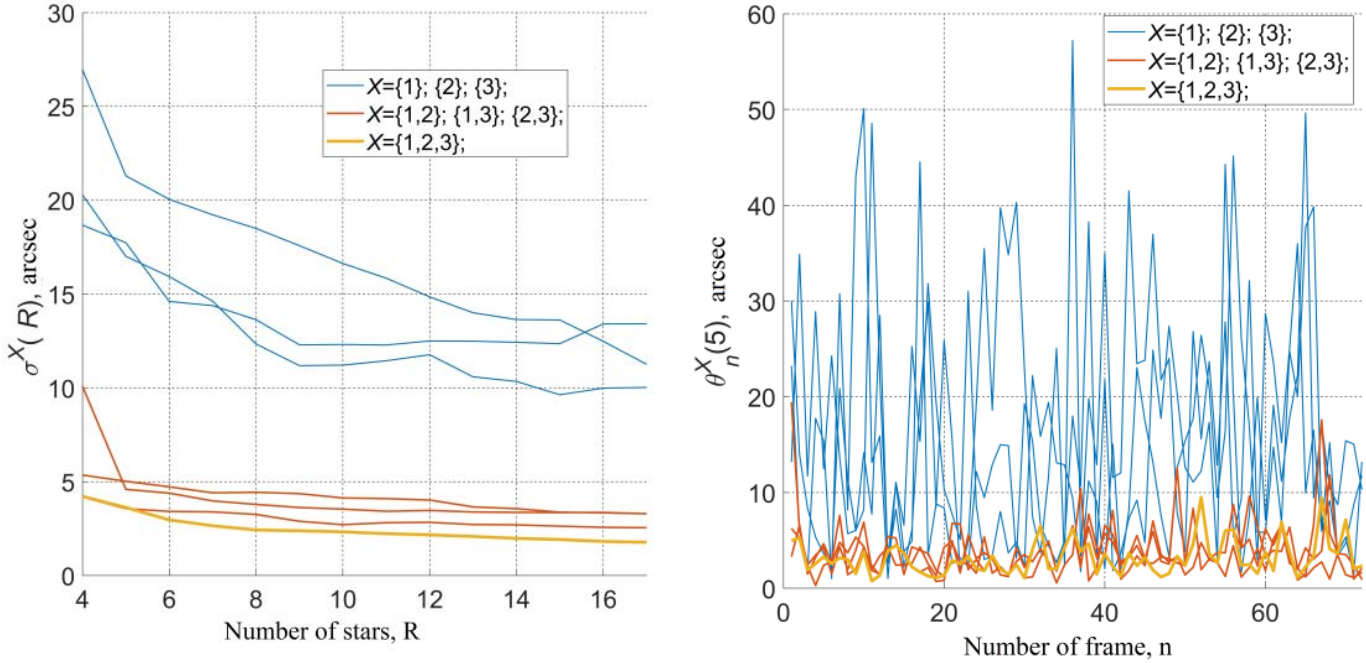

a) *b)*

Fig. 3. AVU attitude errors with different camera configurations: *a)* RMS errors for different numbers of stars R = 4 ... 17 stars; *b)* errors for R = 5 in different frames.

CONCLUSIONS

For an AVU consisting of digital cameras that can stably detect the images of stars up to and including the 10th magnitude, the astronomical calibration of the relative attitude of cameras does not require special calibration test beds. The star calibration observations can be performed even on a fixed base: in this case, the cameras move relative to the observed stars due to the diurnal rotation of the Earth. To process calibration observations, the cameras should be exposed synchronously, and numerical values of moments of time of the start of exposure should be assigned on UTC (SU) time scale. The time scale and coordinates of the calibration site can be obtained from the GNSS (GLONASS) receiver operating in standalone mode. If these conditions are met, the RMS error of camera attitude calibration does not exceed 2 arcsec for the pixel angular size of 13.4 arcsec.

AVU calibration rotations are needed to determine its attitude relative to the IMU measurement basis. As

regards the astronomical calibration of the camera relative attitude, these rotations are optional, but useful. They increase the variation of calibration measurements performed by the AVU due to various parasitic effects. They include the errors in the algorithmic correction of atmospheric refraction and velocity aberration of light in different observation directions and AVU bending deformations in different orientations. Parasitic effects are not explicitly considered in the AVU measurement model, however, they increase the residual error of the system of calibration equations due to a larger variation in the raw calibration measurements. Therefore, the parasitic effects are indirectly taken into account in the AVU calibration results by increasing the calculated values of the variances of explicitly calibrated parameter estimates.

The errors in calibration of the cameras' relative attitude are small; therefore, astronomical observations made by individual cameras can be reduced to a common basis. The observations made with several real cameras can be considered as virtual, i.e., obtained with a single virtual camera with an extended field of view. Virtual observations recognize the detected stars in conditions when each real camera taken separately observes insufficient number of stars. With the same number of detected stars, the calibrated AVU provides a much (5-7 times) smaller attitude error compared to a single camera due to the ability to observe stars with larger angular distances.

An important feature of the considered AVU astronomical calibration algorithm is that it considers refraction and light aberration in the form of nonlinear transformations of the direction vectors of catalog stars projected onto the image plane of the image sensor. These transformations are based on relatively simple models describing a limited number of physical effects. For example, when considering the refraction, the air humidity at the observation point is not taken into account, and when considering the aberration, the addition to the observer's velocity associated with the Earth's diurnal rotation is also omitted. Considering these factors and other macroscopic atmospheric effects may help improve the quality of AVU astronomical calibration.

FUNDING

This work was supported by ongoing institutional funding. No additional grants to carry out or direct this particular research were obtained.

CONFLICT OF INTEREST

The authors of this work declare that they have no conflicts of interest.

REFERENCES

1. Avanesov, G.A., Bessonov, R.V., Kurkina, A.N., Mysnik, E.A., Liskiv, A.S., Lyudomirskiy, M.B., Kayutin, I.S., and Yamshchikov, N.E., Development of autonomous strapdown stellar-inertial navigation system, 19th St. Petersburg International Conference on Integrated Navigation Systems, 2012.
2. Avanesov G.A., Bessonov, R.V., Kurkina, A.N., Ludomirsky, M.B., Kayutin, I.S., and Yamshchikov, N.E., Autonomous strapdown stellar-inertial navigation systems: Design principles, operating modes and operational experience, Gyroscopy and Navigation, 2013, vol. 4, no. 4, pp. 204–215. https://doi.org/10.1134/S2075108713040032
3. Kozlov, A.V., Parusnikov, N.A., Vavilova, N.B., Tarygin, I.E., and Golovan, A.A., Dynamic test bench calibration of strapdown assembled inertial navigation systems, Izvestiya YuFU. Tekhnicheslie nauki, 2018, no. 1, pp. 241–257. https://doi.org/10.23683/2311-3103-2018-1-241-257
4. Avanesov, G.A., Bessonov, R.V., Brysin, N.N., Kurkina, A.N., Liskiv, A.S., Ludomirsky, M.B., Kayutin, I.S., Yamshchikov, N.E., Gavrilov A.L., Gultsov, S.V., and Stepanov, Yu.V., Astroinertial navigation system, Mekhanika, upravlenie i informatika, 2015, vol. 7, no. 2, pp. 21–37.
5. Fedoseev, V.I. and Kolosov, M.P., Optikoelektronnye pribory orientatsii i navigatsii kosmicheskikh apparatov (Optoelectronic Attitude Determination and Navigation Devices for Spacecraft), Moscow: Logos, 2007.
6. Stroilov, N.A., Nikitin, A.V., Kurkina, A.N., and Bessonov, R.V., Cross calibration test bed. Estimating the measurement errors of transformation matrices between the star tracker frames, Proceedings of the 5th All-Russian Scientific and Technical Conference "Sovremennye problemy orientatsii i navigatsii kosmicheskikh apparatov" (Modern Problems in Spacecraft Orientation and Navigation). Series Mechanics, Control, and Informatics, Moscow: Space Research Institute of RAS, 2017, pp. 40–50.
7. Stroilov, N.A., Nikitin, A.V., Kurkina, A.N., Bessonov, R.V., Belinskaya, E.V., and Voronkov, S.V., Methods for ground-based calibration of mutual attitude of star tracker frames, Sovremennye problemy distantsionnogo zondirovaniya Zemli iz kosmosa, 2017, vol. 14, no. 4, pp. 52–66. https://doi.org/10.21046/2070-7401-2017-14-4-52-63
8. Vasilyuk, N. N., Geometric constraints on the accuracy of a vector attitude sensor based on a matrix optical image receiver, Aviakosmicheskoe priborostroenie, 2011, no. 6, pp. 17–24.
9. Blarre, L., Perrimon, N., Majewski, L., and Kocher, Y., HYDRA Multiple Heads Star Tracker based on Active Pixel Sensor and the gyrometer assistance option, 57th International Astronautical Congress, Valencia, Spain, 2006. https://doi.org/10.2514/6.IAC-06-C1.2.10
10. Hua, J., Zhang, T., and Zhu, H., Star image fusion and star recognition of multi-FOV star sensor, Proceedings of 2014 IEEE Chinese Guidance, Navigation and Control Conference, Yantai, China, 2014, pp. 2111–2125. https://doi.org/10.1109/CGNCC.2014.7007502

11. Biryukov, A.V., Prokhorov, M.E., and Tuchin, M.S., Bayesian approach to data fusion in a star tracker with several optical heads, Proceedings of the 6th All-Russian Scientific and Technical Conference "Sovremennye problemy orientatsii i navigatsii kosmicheskikh apparatov" (Modern Problems in Spacecraft Orientation and Navigation). Series Mechanics, Control, and Informatics, Moscow: Space Research Institute of RAS, 2019, pp. 172–185.
12. Zhang, H., Niu, Y., Lu, J., and Yang, Y., Star sensor installation error calibration in stellar-inertial navigation system with a regularized backpropagation neural network, Measurement Science and Technology, 2018, vol. 29, 085102. https://doi.org/10.1088/1361-6501/aac6a8
13. Steffes, S.R., Samaan, M.A., and Theil, S., Alignment between IMU and star tracker using the night sky and an on-board navigation system (AAS 12-042), Guidance and Control 2012: Proceedings of the 35th Annual AAS Rocky Mountain Section Guidance and Control Conference, Breckenridge, Colorado, USA, 2012, Advances in Astronautical Sciences, vol. 144, pp. 173–186.
14. Lu, J., Lei, C., Liang, S., and Yang, Y., An all-parameter system-level calibration for stellar-inertial navigation system on ground, IEEE Transactions on Instrumentation and Measurement, 2017, vol. 66, no. 8, pp. 2065–2073. https://doi.org/10.1109/TIM.2017.2674758
15. Lu, J., Lei, C., and Yang, Y., A dynamic precision evaluation method for the star sensor in the stellar-inertial navigation system, Scientific Reports, 2017, vol. 7, 4356. https://doi.org/10.1038/s41598-017-04061-5
16. Zhang, H., Niu, Y., Lu, J., and Yang, Y., System-level calibration for the star sensor installation error in the stellar-inertial navigation system on a swaying base, IEEE Access, 2018, vol. 6, pp. 47288–47294. https://doi.org/10.1109/ACCESS.2018.2866818
17. Wei, X., Zhang, G., Fan, Q., Jiang, J., and Li, J., Star sensor calibration based on integrated modelling with intrinsic and extrinsic parameters, Measurement, 2014, vol. 55, pp. 117–125. https://doi.org/10.1016/j.measurement.2014.04.026
18. Bessonov R.V., Brysin N.N., Polyansky, I.V., Voronkov, S.V., Belinskaya, E.V., Polishchuk, G.S., Tregub, V.P., and Zavgorodniy, D.S., Test bed equipment for determining the optical characteristics of star trackers, Proceedings of the 5th All-Russian Scientific and Technical Conference "Sovremennye problemy orientatsii i navigatsii kosmicheskikh apparatov" (Modern Problems in Spacecraft Orientation and Navigation). Series Mechanics, Control, and Informatics, Moscow: Space Research Institute of RAS, 2017, pp. 51–60.
19. The Hipparcos and Tycho Catalogues, European Space Agency, 1997.
20. Vasilyuk, N.N., Vector correction of atmospheric refraction for an intra-atmospheric stellar orientation sensor, Aviakosmicheskoe priborostroenie, 2022, no. 9, pp. 31–44. https://doi.org/10.25791/aviakosmos.9.2022.1299.
21. Vasilyuk, N.N., Vector correction of velocity aberration for an intra-atmospheric stellar orientation sensor, Aviakosmicheskoe priborostroenie, 2022, no. 10, pp. 17–31. https://doi.org/10.25791/aviakosmos.10.2022.1302.
22. Garanin, S.G., Zykov, L.I., Klimov, A.N., Kulikov, S.M., Smyshlyaev, S.P., Stepanov, V.V., and Syundyukov, A.Yu., Daytime observation of low-brightness stars (7m-8m) from level terrain, Journal of Optical Technology, 2017, vol. 84, no. 12, pp. 816–821. https://doi.org/10.1364/JOT.84.000816
23. Lukin, V.P. and Nosov, V.V., Measurement of jitter of an extended incoherent radiation source image, Kvantovaya elektronika, 2017, vol. 47, no. 6, pp. 580–588.
24. Tan, W., Dai, D., Wu, W., Wang, X., and Qin, S., A comprehensive calibration method for a star tracker and gyroscope units integrated system, Sensors, 2018, vol. 18, no. 9, 3106. https://doi.org/10.3390/s18093106
25. Yang, Z., Zhu, X., Cai, Z., Chen, W., and Yu, J., A real-time calibration method for the systematic errors of a star sensor and gyroscope units based on the payload multiplexed, Optik, 2021, vol. 225, 165731. https://doi.org/10.1016/j.ijleo.2020.165731
26. Singla, P., Griffith, D.T., Katake, A., and Junkins, J.L., Attitude and interlock angle estimation using split-field-of-view star tracker, Journal of the Astronautical Sciences, 2007, vol. 55, no. 1, pp. 85–105. https://doi.org/10.1007/BF03256516
27. Somov, E.I. and Butyrin, S.A., Flight calibration and adjustment of the astroinertial system determining the attitude of a maneuvering Earth observation satellite, Izvestiya Samarskogo nauchnogo tsentra Rossiiskoi akademii nauk, 2016, vol. 18, no. 4-6, pp. 1128–1137.
28. Somov, E.I. and Butyrin, S.A., Digital signal processing in an astroinertial system for determining attitude and angular rate of a maneuvering land-survey satellite, 24th St. Petersburg International Conference on Integrated Navigation Systems, 2017. Pp 559-563.
29. Jiang, J., Yu, W., and Zhang, G., High-accuracy decoupling estimation of the systematic coordinate errors of an INS and intensified high dynamic star tracker based on the Constrained Least Squares Method, Sensors, 2017, vol. 17, no. 10, 2285. https://doi.org/10.3390/s17102285
30. Vasilyuk, N.N., Star tracker error model taking into account the calibration errors of intrinsic parameters of the digital camera, Gyroscopy and Navigation, 2024, vol. 15, no. 1. Pp 31-59.
31. Vasilyuk, N.N., Nefedov, G.A., Sidorova, E.A., and Shagimuratova, N.O., Calibration of the intrinsic parameters of the digital camera of a star tracker based on ground-based observations of stars, taking atmospheric refraction and aberration of light into account, Measurement Techniques, 2023, vol. 66, no. 8, pp. 593–609. https://doi.org/10.1007/s11018-023-02272-z
32. RD 50-25645.325-89. Methodological guidelines. Earth's artificial satellites. Main coordinate systems for ballistic flight support and methods for calculating sidereal time.
33. Mudrov, V.I. and Kushko, V.L., Metody obrabotki izmerenii. Kvazipravdopodobnye otsenki (Measurement Processing Methods. Quasi-likelihood Estimates), Moscow: Radio i Svyaz', 1983, second edition.
34. Markley, F.L., Attitude determination using vector observations and the singular value decomposition, Journal of the Astronautical Sciences, 1988, vol. 36, no. 3, pp. 245–258.